

Extracting Spectral Index of Intergalactic Magnetic Field from Radio Polarizations

Prabhakar Tiwari^a and Pankaj Jain^b

^a *Technion - Israel Institute of Technology, Haifa - 3200003, Israel*

^b *Department of Physics, Indian Institute of Technology, Kanpur - 208016, India*

ABSTRACT

We explain the large scale correlations in radio polarization in terms of the correlations of primordial/source magnetic field. The radio waves are dominantly produced by the synchrotron mechanism and hence their polarization angle is deemed to be correlated with the magnetic field of the radio source. The primordial intergalactic magnetic field seeds the source magnetic field and hence it is possible that during the source evolution the correlations of primordial magnetic field survived. We model the intergalactic magnetic field in all 3D space and fit its correlations with JVAS/CLASS radio polarization alignments. We find that the radio polarization alignments are best fitted with the magnetic field spectral index given by -2.43 ± 0.02 . We show that primordial magnetic field correlation provides a good explanation of the observed radio polarization alignment.

Subject headings: polarization, galaxies: high-redshift, galaxies: active

1. Introduction

The polarization directions from distant radio sources have been observed to show an alignment over a distance scale of order 150 Mpc (Tiwari & Jain 2013). This alignment is seen in the significantly polarized sources in JVAS/CLASS data (Jackson et al. 2007) with polarized flux greater than 1 mJy. The explanation for such large scale alignment, however, remains puzzling till date. This paper is an attempt to explain these alignments.

The radiation from the radio sources is dominantly synchrotron and so the polarization properties of radio sources are most likely determined by the magnetic environment at the source. The magnetic field corresponding to the large scale structures, with distance scales of order 150 Mpc, is expected to be stronger than intergalactic magnetic field on larger distance scales. Furthermore, the source magnetic field is responsible for the synchrotron emission and hence would be correlated with the radio polarizations. An interesting possibility is that the source magnetic field is also correlated with the orientation of the galaxies. This would imply a correlation between the galaxy orientation and the radio polarizations. The seed magnetic field of a radio source is expected to arise from the primordial intergalactic magnetic field. As the source evolves, it's magnetic field gets enhanced and may eventually loose large scale correlations. However, there is a possibility that these correlations

are not lost entirely. The observed polarization alignment at 150 Mpc provides a good motivation to consider this hypothesis. Another very interesting observation which supports this hypothesis is the observed correlation between quasar polarizations and large-scale structures (Hutsemékers et al. 2014).

Here we propose a simple theoretical model to describe the statistical properties of the radio polarization angles of sources within a cluster. We propose that the polarization angle of the source is perfectly correlated with the background cluster magnetic field. The background magnetic field is assumed to have the same statistical properties as the primordial magnetic field (Subramanian et al. 2003; Seshadri & Subramanian 2005, 2009; Jedamzik et al. 1998; Subramanian & Barrow 1998). It is parametrized in terms of its strength and the spectral index. This provides us with a simple model for the statistical correlations among the polarization angles. We next fit this model to the observed radio polarizations in order to determine spectral index. We use the significantly polarized sources, that is, sources which have polarized flux greater than 1 mJy, for this fit. Since the correlation between the polarizations and magnetic field is not expected to be perfect, the fit might be interpreted as the lower limit on the spectral index of the magnetic field. In any case, we find that the statistical model provides a good fit to the polarization data.

The paper is organized as follows. In Sec. 2 we describe the magnetic field model and explain its correlations in real space. We also explain our numerical procedure to generate a full 3D realization of magnetic field for a particular set of parameters. In Sec. 3 we give details of the JVAS/CLASS data and discuss the observed alignments. In Sec. 4 we review different statistical measures of alignment used in this paper. We describe our procedure in Sec. 5. We present our results in Sec. 6 and conclude in Sec. 7.

2. Correlations in Inter-Galactic Magnetic Field

Magnetic field has been observed at all scales in inter-galactic medium. However the origin of observed magnetic field is unknown and most likely to be primordial (Subramanian et al. 2003; Seshadri & Subramanian 2005, 2009; Jedamzik et al. 1998; Subramanian & Barrow 1998). Here we assume that the intergalactic magnetic field within a cluster has statistical properties similar to those of the primordial field. However its strength and spectral index may be different. Let $b_i(\vec{k})$ represent the magnetic field in Fourier space. We can express its two point correlations as,

$$\langle b_i^*(\vec{k}) b_j(\vec{q}) \rangle = \delta_{\vec{k}, \vec{q}} P_{ij}(\vec{k}) M(k) \quad (1)$$

where $k = |\vec{k}|$ and P_{ij} is the projection operator given as,

$$P_{ij} = \left(\delta_{ij} - \frac{k_i k_j}{k^2} \right), \quad (2)$$

The real space magnetic field can be written as,

$$B_i(\vec{r}) = \frac{1}{V} \sum_k b_i(\vec{k}) e^{i\vec{k}\cdot\vec{r}} \quad (3)$$

where V is the volume. We assume a power law dependence of the spectral function $M(k)$

$$M(k) = Ak^{n_B}, \quad (4)$$

with the spectral index $n_B > -3$. The magnetic field is assumed to be statistically uncorrelated in k -space. However the field is correlated in real space and the nature of correlation is controlled by the index n_B . We can write the real space correlation of the field as the Fourier transform of Eq. 1. We obtain,

$$\langle B_i(\vec{r} + \vec{r}') B_j(\vec{r}) \rangle = \frac{1}{V} \int d^3k e^{i\vec{k}\cdot\vec{r}'} P_{ij}(\vec{k}) M(k) W^2(kr_G), \quad (5)$$

where r_G is the "galactic" scale taken as 1 Mpc and W is a window function of the form,

$$W(x) = \begin{cases} 1 & x < 1 \\ 0 & x > 1 \end{cases} \quad (6)$$

This window function fixes the value of the scale r_G . The magnetic field $B(\vec{r})$ is assumed to be uniform over the scale $r_G = k_G^{-1} = 1$ Mpc. In Eq. 5 we have also taken the continuum limit and replaced \sum_k by $\frac{1}{V} \int d^3k$. The constant A in Eq. 4 is equal to $V\pi^2 B_0^2 \frac{3+n_B}{k_G^{3+n_B}}$. It is fixed by demanding $\sum_k \langle B_i(\vec{r}) B_i(\vec{r}) \rangle = B_0^2$, where B_0 is the intergalactic magnetic field averaged over the distance scale of $r_G = 1$ Mpc. We expect that $B_0 \sim \text{nG}$ (Seshadri & Subramanian 2009; Yamazaki et al. 2010; De Angelis et al. 2008), although this value plays no role in our analysis.

It is also appropriate to demand a large scale cut-off for the correlations in Eq. 5. Here we assume that this cutoff is sufficiently large ($r_{max} > 3\text{Gpc}$) so that we can simply set r_{max} to be ∞ . Hence, we set the lower limit of integration in Eq. 5 as $k_{min} = r_{max}^{-1} = 0$. We emphasize that such large scale correlations are within the Big-Bang cosmology. The perturbation at the time of inflation have wavelengths larger than the comoving size of the current observable universe and hence the primordial magnetic field correlations may also exist over the horizon scale.

We numerically generate intergalactic magnetic field in $3D$ space using the procedure described in (Agarwal et al. 2012) for different values of the spectral index n_B . We consider discretized space consisting of a large number of cells or domains of equal size. The magnetic field is assumed to be uniform in each domain. We first generate the magnetic field in k -space, which is straightforward since the corresponding field is uncorrelated. It is convenient to use polar coordinates (k, θ, ϕ) in k -space. The projection operator $P_{ij}(\vec{k})$ ensures that the component of magnetic field along \vec{k} , b_k is zero. The remaining two orthogonal component b_θ and b_ϕ are uncorrelated and therefore we generate these by assuming the Gaussian distribution,

$$f(b_\theta(\mathbf{k}), b_\phi(\mathbf{k})) = N \exp \left[- \left(\frac{b_\theta^2(\mathbf{k}) + b_\phi^2(\mathbf{k})}{2M(\mathbf{k})} \right) \right], \quad (7)$$

where N is the normalization. The distribution in Eq. 7 represents an uncorrelated magnetic field in k -space. Next, we do a Fourier transform to obtain magnetic field in real space.

3. Data

We use the catalogue produced by Jackson et al. (2007). The catalogue contains 12743 core dominated flat spectrum radio sources and provides their angular coordinates and the Stokes I , Q and U parameters. Many of these sources are located at very large distances. However, the redshift for most of these sources is unknown. The observable required for the alignment study is the polarization angle. A detailed description of the catalogue including the calibration methods is given in Jackson et al. (2007).

A signal of alignment of radio polarization angles has been found in significantly polarized sources, with polarized flux greater than 1 mJy, contained in this catalogue (Tiwari & Jain 2013). The alignment was seen over the distance scales of order 150 Mpc. At larger distances the authors (Tiwari & Jain 2013) do not find a significant signal of alignment and confirm the earlier null result in (Joshi et al. 2007). A recent study of this data with an alternate statistical measure also indicates alignment in data (Shurtleff 2014). Furthermore alignments have been found even at larger distances for QSOs in this data sample (Pelgrims & Hutsemékers 2015).

We find that there are 4400 sources in catalogue with polarized flux greater than 1 mJy. We further remove 187 sources from these 4400 sources as their angular positions coincide with other sources. We point out that the sources lie dominantly in the Northern hemisphere. Furthermore there are very few sources along the galactic plane. We use only this sample of 4213 sources for our analysis.

The alignment statistic we use is defined for the number of nearest neighbours, n_v , a proxy for distance. In order to relate n_v to distance we assume that all sources are located at redshift equal to unity. We need to make this assumption since the redshift information of most sources is not currently available. In any case most sources are known to be located at very large distances and hence this assumption is reasonable. We show the relationship between the average comoving distance and n_v in Fig. 1. The standard Lambda Cold Dark Matter model is used for computing the comoving distance (Weinberg 2008). Independently we also use a statistic which considers alignment of a source with all sources located within a fixed radius.

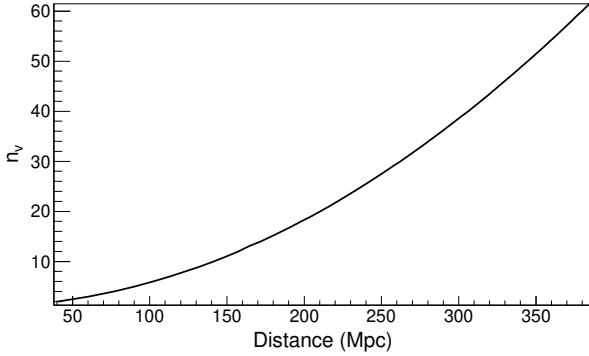


Fig. 1.— The number of nearest neighbours (n_v) as a function of the mean distance (Mpc) among sources for data with polarization flux greater than 1 mJy.

4. Correlation Statistic

In order to quantify the correlations between polarizations at different positions we define two statistics, S_D and S'_D . Let us consider the n_v nearest neighbours of the source at site k . Let ψ_i be the polarization angle of the source at the i^{th} site within this set. The dispersion of polarization angles in the neighbourhood of this site may be characterized by the measure,

$$d_k = \frac{1}{n_v} \sum_{i=1}^{n_v} \cos[2(\psi_i + \Delta_{i \rightarrow k}) - 2\psi_k]. \quad (8)$$

Here the factor $\Delta_{i \rightarrow k}$ arises since the polarizations at two different points, labelled as i and k , on the celestial sphere have to be correlated after making a parallel transport from $i \rightarrow k$ (Jain et al. 2004) along the geodesic which connects the two positions. The parameter ψ_k in this equation is the polarization angle at the site k . The measure d_k provides an estimate of the dispersion. We point out that a large value of d_k implies low dispersion and vice versa. The statistic is defined as (Hutsemékers 1998; Jain et al. 2004),

$$S_D = \frac{1}{n_s} \sum_{k=1}^{n_s} d_k, \quad (9)$$

where n_s is the total number of data samples. A strong alignment between polarization vectors implies a large value of S_D . We point out that the notation used here is a little different from that used in Tiwari & Jain (2013).

We also use an alternate statistic S'_D where we measure the dispersion over a fixed distance d_v . Let n_k be the number of sources in the neighbourhood of the k^{th} site within the fixed distance d_v . This number will of course depend on the site. The measure of dispersion at any site is given as,

$$d'_k = \frac{1}{n_k} \sum_{i=1}^{n_k} \cos[2(\psi_i + \Delta_{i \rightarrow k}) - 2\psi_k]. \quad (10)$$

The variables, ψ_i , $\Delta_{i \rightarrow k}$ and ψ_k in Eq. 10 are same as in Eq. 8. A large value of d'_k implies low dispersion and vice versa within a circle of fixed radius d_v . Now, the statistic is given by the average over all sources n_s ,

$$S'_D = \frac{1}{n_s} \sum_{k=1}^{n_s} d'_k, \quad (11)$$

We point out that these two statistic S_D and S'_D will give same result for a spatially uniform source distribution since for a circle of a given radius the nearest number of sources will be same everywhere. Hence, S_D can be translated into S'_D naively. However, the data sample is expected to show some deviation from spatial uniformity and hence we expect small differences in the two measures, S_D and S'_D .

5. Procedure

We first determine the statistic S_D (Eq. 9) for the observed linear polarization angles. The same procedure is repeated for the theoretical polarization angles, which are assumed to be aligned perpendicular to the background magnetic field. The magnetic field is generated by simulations as explained in section 2. The resulting theoretical values of S_D are computed for a range of values of the spectral index n_B . The best fit value of n_B is obtained by making a χ^2 fit to the observed data.

In order to compute χ^2 we need an estimate of the error in the statistic S_D . Here we make a rough estimate by assuming that each polarization angle has a statistical error of $\delta\psi \approx 10^\circ$. We do not include systematic errors in our analysis, mainly because their value is not known. The error in the value of the statistic S_D can be approximated by assuming that all terms in the sum in Eq. 9 are independent of one another. Furthermore we assume that d_k is approximately independent of k . The error in S_D is then given by, $\delta S_D \approx \delta d_k / \sqrt{n_s}$. The error in d_k is found to be

$$\delta d_k \leq \frac{1}{n_v} \sum_{i=1}^{n_v} 2\delta\psi_i \quad (12)$$

Assuming that the errors in different polarization angles is uncorrelated we obtain $\delta d_k \approx 2\delta\psi / \sqrt{n_v}$. Here we have assumed the maximum error in δd_k . The error in S_D is, therefore,

$$\delta S_D = 2\delta\psi / \sqrt{n_s n_v}. \quad (13)$$

It is clear that our assumption that different terms in the sum in Eq. 9 are independent of one another is not really correct since a particular polarization angle contributes to d_k values at different sites. Also we only consider relatively small values of $\sqrt{n_v} \leq 10$. Hence, due to these uncertainties, above error estimates are reliable only up-to a factor or order unity. We test above estimate (Eq.13) and obtain true error in S_D by direct simulations. We assume random error of 10° in all polarization angles and calculate S_D for 1000 realizations. As expected, a Gaussian provides a good fit to the

simulated S_D distribution. We can obtain an estimate of the error δS_D from the fitted sigma value. The distribution of S_D and a Gaussian fit for $n_v = 10$ is shown in Fig. 2. The estimated value of δS_D is found to be 0.002, which is comparable but somewhat larger than our estimate. This is reasonable since our analytic expression for error, Eq. 13, is expected to be an underestimate since we have assumed that the different terms in the sum in Eq. 12 are uncorrelated. This is not really correct. We show all the simulated δS_D in Fig. 3. The analytic estimate is also shown for comparison. We similarly calculate the error for statistics S'_D . The corresponding results are shown in Fig. 4. For comparison we have converted the distance in this case to the averaged number of nearest neighbours n_v .

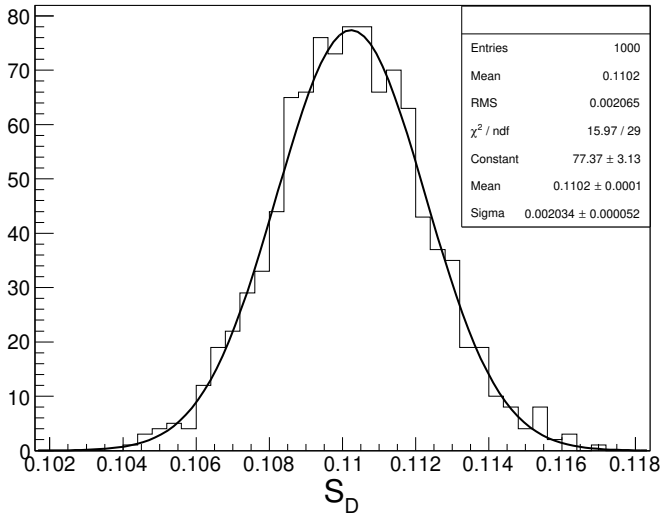


Fig. 2.— S_D distribution after adding normal random error of 10° in all polarization angles. Here we have set $n_v = 10$.

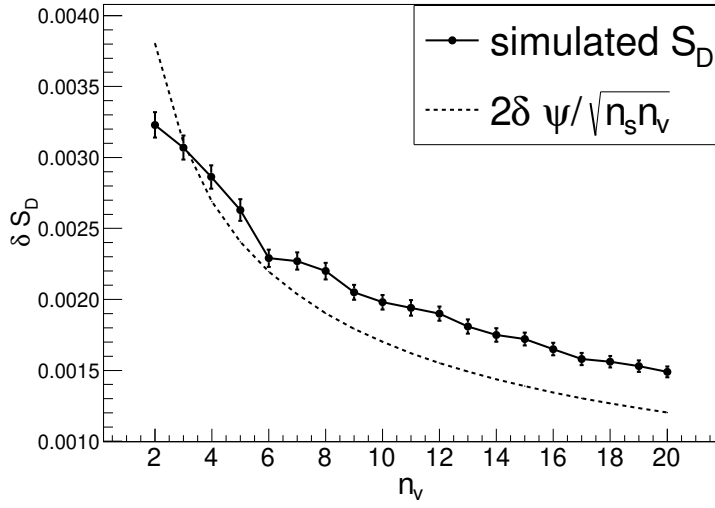


Fig. 3.— Estimated and simulated δS_D . The simulation is done by adding normal random error of 10° in all polarization angles. The error bars are the errors in fitted δS_D (Fig. 2).

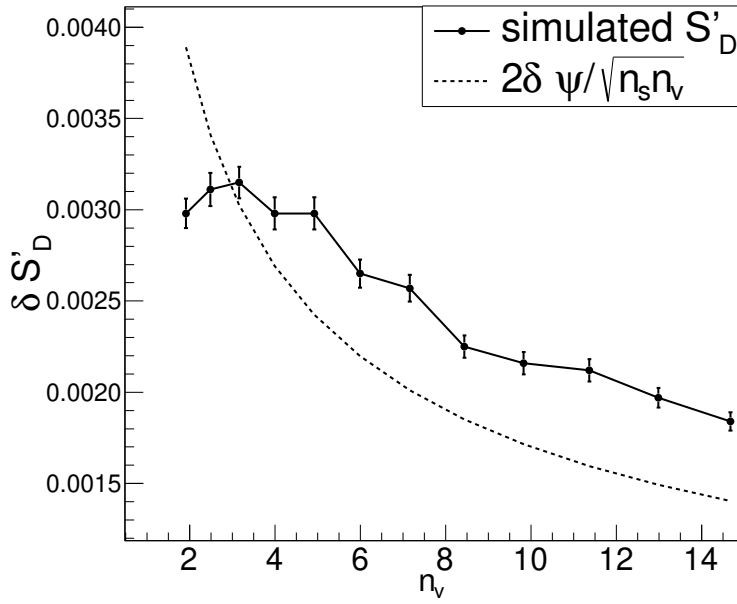


Fig. 4.— Estimated and simulated $\delta S'_D$. The simulation is done by adding normal random error of 10° in all polarization angles. The error bars are the errors in fitted $\delta S'_D$.

6. Results

The simulated S_D values for different n_B are fitted with observed data S_D , whereas the error in data S_D is directly computed by simulation assuming 10° random error in polarization angles. The χ^2 for different n_B is computed as,

$$\chi^2 = \sum_{n_v=2}^{10} \left(\frac{S_D(\text{observed}) - S_D(\text{simulated})}{\delta S_D} \right)^2, \quad (14)$$

where δS_D is the error in $S_D(\text{observed})$ (see Fig. 3). We similarly calculate χ^2 for S'_D . The maximum value of n_v is set equal to 10. This choice is made since the significance of alignment starts to decrease beyond $n_v = 10$ and it is not found to be significant for $n_v > 11$. With one parameter the number of degrees of freedom (DOF) is equal to eight. We present the χ^2/DOF values versus spectral index n_B for statistic S_D in Fig. 5. The minimum value of χ^2/DOF is found to be approximately 4.5 at $n_B = -2.51$. The data and best fitted simulated S_D comparison for spectral index $n_B = -2.51$ is given in Fig. 7. Including one sigma error, the extracted value of n_B is found to be, $n_B = -2.51 \pm 0.01$. We point out that the relatively high value of χ^2 might be an indication that the power law does not provide the best fit to the data. Alternatively it is possible that the errors might have been underestimated. In particular, we have not included systematic errors in our analysis. Furthermore, we have assumed a perfect alignment of polarization angles with the magnetic field, whereas in reality this assumption may not be true. This implies that the model needs to be generalized further. Here we ignore these complications and confine ourselves to the simple model which assumes perfect correlations. The extracted absolute magnitude of n_B in this case may be interpreted as its lower limit.

The results for the case of the alternate statistic S'_D are shown in Fig. 6. In this case we set the maximum value of the fixed distance d_v is set equal to 201 Mpc. This value is chosen since for this case the mean number n_v of nearest neighbours is equal to 10. Hence this value is chosen in order to be compatible with the results obtained by the statistic S_D . We point out that for a fixed distance of 201 Mpc, the mean value of n_v is 10 whereas if we fix the value of n_v for each source to be 10, the mean distance is found to be 150 Mpc. This difference arises due to non-uniformity in the distribution of sources and is likely to lead to some difference in the extracted value of n_B using the two different statistics.

In the case of the statistic S'_D , the minimum value of χ^2/DOF is found to be 5.7 corresponding to $n_B = -2.43 \pm 0.02$. The χ^2 values in Fig. 6 show a relatively larger dependence on n_B and hence lead to a larger error. The difference in the extracted values of n_B for the two statistics reflects the spatial non-uniformity of data. More uniform data is needed to settle the differences in statistics and to fix the value of n_B more accurately. The value extracted using the statistic S'_D may be more reliable since it includes sources within a fixed distance from a particular source rather than including a fixed number of nearest neighbours. Also higher value of n_B is expected as the source evolution is more likely to kill some correlations. Furthermore, as argued above our analysis may be interpreted as providing a lower limit on the magnitude of n_B . Since the absolute magnitude of

n_B extracted from S'_D is lower than that extracted by using S_D , we consider the former value as a more reliable lower limit.

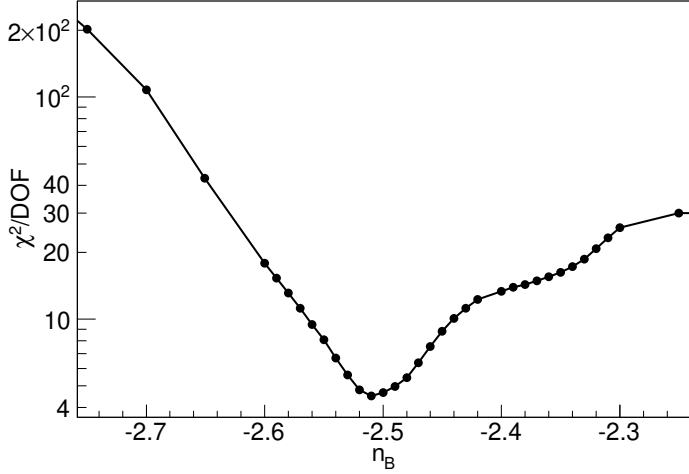


Fig. 5.— The χ^2/DOF versus spectral index n_B for the S_D fit up to $n_v \leq 10$.

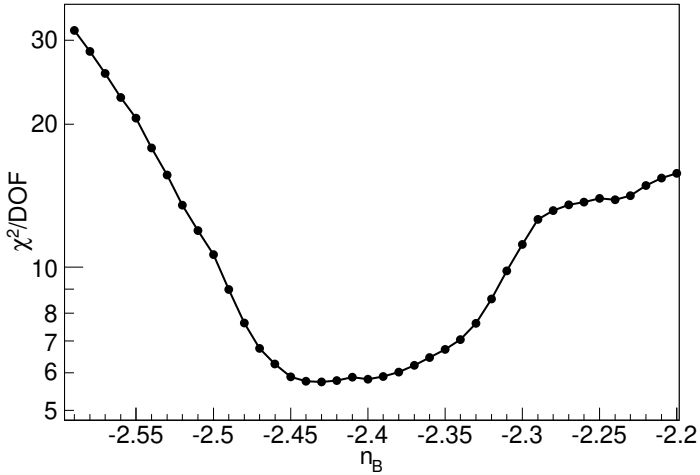


Fig. 6.— The χ^2/DOF versus spectral index n_B for S'_D fit up to the fixed distance $d_v \leq 200$ Mpc.

A comparison with real data statistic S_D and our proposed model statistic is given for the best fitted n_B in Fig. 7.

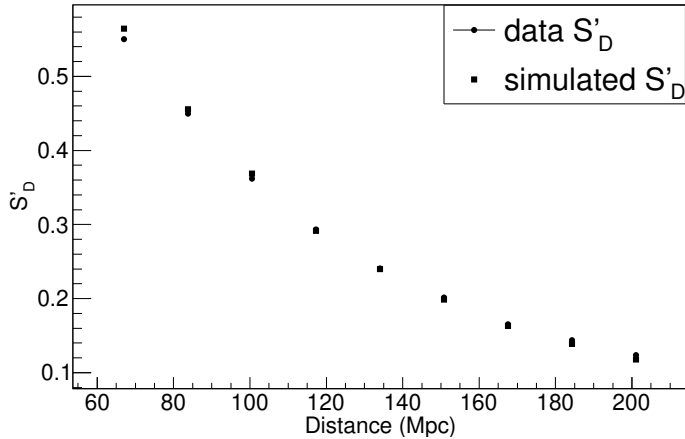


Fig. 7.— The statistic S'_D for the real data and simulated polarization from the background magnetic field at the source. This is for the best fitted spectral index $n_B = -2.43$. The error bars in S'_D are very small, most of the time less than the size of marker itself. We have translated the number of nearest neighbour into distance.

7. Conclusion

We have presented a possible model to explain the large scale polarization radio correlations. Here, we only analyse the JVAS/CLASS data and show that the observed alignment can be successfully explained as magnetic field correlations. The model can be further applied to other data sets and tested. We conclude that the best fit of the spectral index from the JVAS/CLASS radio data indicates that $n_B \leq -2.43 \pm 0.02$.

Acknowledgements

We have used CERN ROOT 5.27 for generating our plots.

REFERENCES

- Agarwal, N., Aluri, P. K., Jain, P., Khanna, U., & Tiwari, P. 2012, Euro. Phys. Jour. C, 72, 15
- De Angelis, A., Persic, M., & Roncadelli, M. 2008, Mod. Phys. Lett., A23, 315
- Hutsemékers, D. 1998, A&A, 332, 410
- Hutsemékers, D., Braibant, L., Pelgrims, V., & Sluse, D. 2014, A&A, 572, A18
- Jackson, N., Battye, R., Browne, I., et al. 2007, MNRAS, 376, 371

- Jain, P., Narain, G., & Sarala, S. 2004, MNRAS, 347, 394
- Jedamzik, K., Katalinic, V., & Olinto, A. V. 1998, Phys. Rev., D57, 3264
- Joshi, S., Battye, R., Browne, I., et al. 2007, MNRAS, 380, 162
- Pelgrims, V., & Hutsemékers, D. 2015, arXiv:1503.03482
- Seshadri, T. R., & Subramanian, K. 2005, Phys. Rev., D72, 023004
- . 2009, Phys. Rev. Lett., 103, 081303
- Shurtleff, R. 2014, arXiv:1408.2514
- Subramanian, K., & Barrow, J. D. 1998, Phys. Rev., D58, 083502
- Subramanian, K., Seshadri, T. R., & Barrow, J. D. 2003, MNRAS, 344, L31
- Tiwari, P., & Jain, P. 2013, Int. J. Mod. Phys., D22, 1350089
- Weinberg, S. 2008, Cosmology (Oxford University Press)
- Yamazaki, D. G., Ichiki, K., Kajino, T., & Mathews, G. J. 2010, Phys. Rev., D81, 023008